POLITECNICO DI TORINO
Repository ISTITUZIONALE

Impact of Parameters Variability on the Electrical Performance of Carbon Nanotube Interconnects

Original
Impact of Parameters Variability on the Electrical Performance of Carbon Nanotube Interconnects / Stievano, IGOR SIMONE; Manfredi, Paolo; Canavero, Flavio. - STAMPA. - (2011), pp. 83-86. (Intervento presentato al convegno 15th IEEE Workshop on Signal Propagation on Interconnects tenutosi a Napoli (I) nel May 8-11, 2011).

Availability:
This version is available at: 11583/2422537 since:

Publisher:

Published
DOI:

Terms of use:

This article is made available under terms and conditions as specified in the corresponding bibliographic description in the repository

Publisher copyright

(Article begins on next page)

12 October 2024

Impact of Parameters Variability on the Electrical Performance of Carbon Nanotube Interconnects

I. S. Stievano, P. Manfredi, F. G. Canavero
Dip. Elettronica, Politecnico di Torino, Italy (igor.stievano@polito.it)

Abstract

This paper addresses the simulation of carbon nanotube interconnects with the inclusion of the effects of parameter uncertainties due to the fabrication process. The proposed approach is based on the available state-of-the-art models of nanointerconnects and on the expansion of the voltage and current variables in terms of orthogonal components, leading to an enhanced stochastic model. The method offers comparable accuracy and improved efficiency in computing parameters variability effects on system responses with respect to conventional methods like Monte Carlo. A realistic application example involving the frequency-domain analysis of an high-speed nanointerconnect concludes the paper.

1 Introduction

Over the last ten years, the interest in new materials and design solutions for the development of high-performance interconnects for nanoelectronic applications has grown. With the shrinking of the physical dimension of devices in the nanoscale range, the traditional copper interconnects exhibit large resistivity and poor current density and demand for the availability of alternative solutions. Carbon nanotubes (CNT) provide a well known example of this trend. They offer exceptional mechanical and electrical properties and represent a good candidate for replacing copper for future VLSI applications [1, 2, 3].

Within this framework, numerical models of CNT interconnects are required for assessing strengths and limitations of application designs implementing this technology. The recent literature proposed a number of models for the description of the electromagnetic behavior of CNT structures. Without loss of generality, we limit ourselves to the results based on the approximation of signal propagation on nanointerconnects via the well-known telegraph equations (e.g., see [2, 4, 5, 6] and references therein). The proposed models rely on the transmission line theory and allow to simulate realistic nanointerconnects in either the frequency- and the time-domain via standard techniques [7]. However, the main limitation of the available approaches is that the proposed CNT models are deterministic, i.e., they describe a nanostructure with predefined values of its electrical and geometrical parameters. The effects of the uncertainties of circuit parameters possibly due to temperature or tolerances of the manufacturing process, need to be taken into account for the realistic prediction of the system performance.

The aim of this paper is the extension of the state-of-the art transmission-line models of a CNT interconnect to account for the inherent variability of model parameters. The proposed method is based on the so-called Polynomial Chaos (PC) theory, that assumes a series of orthogonal polynomials of random variables for the solution of a stochastic problem [8][1]. This technique has been successfully applied to several problems in different domains, including the extension of the classical circuit analysis tools, like the modified nodal analysis (MNA), to the prediction of the stochastic behavior of circuits [10]. Recently, the authors extended the results to long distributed interconnects described by multiconductor transmission-line equations [11]. The advocated method turns out to be much faster than alternate available solutions for variability, like Monte Carlo simulation, while maintaining comparable accuracy.

2 CNT bundles

The basic building structure of a CNT interconnect is represented by a single-walled carbon nanotube (SWCNT) (i.e., a mono-atomic layer of graphite). A SWCNT has a diameter on the order of few nanometers and can exhibit either a semiconducting or a metallic behavior depending on the way it is rolled-up. Due to the manufacturing process, the interconnect is obtained by the parallel connection of a bundle of SWCNTs as shown in the cross-section Fig. 1. The above configuration reduces the intrinsic high resistive behavior of a single conductor and allows that a sufficient number of CNTs (approximately one third) behave as metallic conductors.

Of course, this is not the only possibility and some alternative solutions are currently under study. An example is provided by the so-called multi-wall carbon nanotubes (MWCNTs) consisting of several graphene sheets arranged in a coaxial configuration.

For the sake of simplicity, the results of this study are based on the SWCNT bundle of Fig. 1. However, they are general and can be readily applied to alternative configurations.

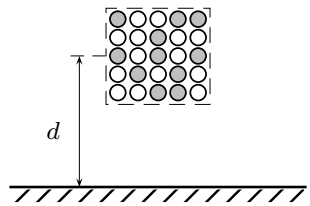

Figure 1: Cross-section of a typical nanointerconnect composed of a bundle of SWCNTs in horizontal configuration, above the ground plane. The gray circles correspond to the conducting nanotubes.

3 Simplified equivalent model

This Section briefly provides an overview of the available results for the modeling of the signal propagation on the bundle of Fig. 1. A detailed discussion of model derivation and validity is out of the scope of this paper and readers are referred to [2, 3, 4, 5, 6].

[1] In this context, the word Chaos is used in the sense originally defined by Wiener [9] as an approximation of a Gaussian random process by means of Hermite polynomials.

Under specific conditions, a single CNT above a ground plane behaves as an RLC transmission line with a suitable definition of the per-unit-length parameters. Specifically, both the inductance and the capacitance of the line are made of two contributions. The classical magnetic inductance and electrostatic capacitance are combined with two new parameters, namely the so-called *kinetic inductance* L_k and *quantum capacitance* C_q, given by

$$L_k = \frac{h}{8e^2\nu_F}, \quad C_q = \frac{8e^2}{h\nu_F} \tag{1}$$

where $h = 6.626 \times 10^{34}$ is the Plank constant, $e = 1.602 \times 10^{19}$ C is the electric charge carried by a single electron and ν_F is the *Fermi velocity*. For the case of graphene, $\nu_F \approx 8 \times 10^5$ m/s and the above parameters become $L_k = 4\,\mathrm{nH}/\mu\mathrm{m}$ and $C_q = 0.4$ aF/nm. It is worth noticing that the magnetic inductance is much lower than the kinetic inductance and hence can be neglected in modeling CNT interconnects. The losses are described by the per-unit-length parameter R' and two identical lumped series resistors $R_p/2$ that are independent of the line length and account for the intrinsic quantum resistance of a nanotube. The above parameters write

$$R_p = h/4e^2, \quad R' = R_p/2\lambda_{\mathrm{mfp}} \tag{2}$$

where λ_{mfp} is the *mean-free-path* of free electrons. In the low bias condition, i.e., for a longitudinal electric field less than 0.16 V/m, it is on the order of 1 μm. The intrinsic resistance is $R_p = 6.45\,\mathrm{k}\Omega$.

Based on the previous considerations, when the SWCNTs are arranged in a bundle, the circuit equivalent of the nanointerconnect is the multiconductor transmission-line shown in Fig. 2. In this case, the quantum and kinetic parameters become diagonal matrices since experimental and theoretical studies have demonstrated that electron transport along one tube of the bundle is weakly affected by the presence of nearby SWCNTs. On the contrary, the alternate classical electrostatic and magnetic matrices become full matrices that accounts for the interaction among the conductors and that can be computed via standard analytical formulas or numerical methods.

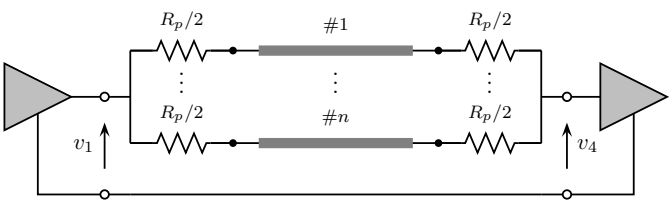

Figure 2: Multiconductor model of the SWCNT bundle of Fig. 1. This scheme represents the typical configuration of a nanointerconnect used as an high-speed link between a driver and a receiver.

However, since the nanotubes are short-circuited at both ends, the RLC transmission-line equivalent of Fig. 3 is often used [5, 6]. This simplified model unavoidably introduces some approximations but is much simpler than the one of Fig. 2 and requires less information for the computation of model parameters. It can be derived by assuming identical currents flowing into the different terminals of the multiconductor transmission-line of Fig. 2. Also, even if the equivalent capacitance C_e can be obtained from the full electrostatic per-unit-length capacitance matrix of the structure of Fig. 2 (e.g., see [5]), approximate formulas are commonly used, as the analytical per-unit-length capacitance of a wire above a ground plane [7].

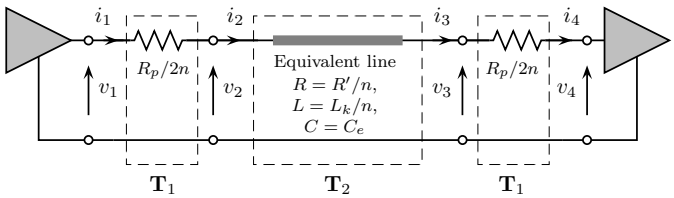

Figure 3: Simplified equivalent RLC transmission-line of a CNT interconnect.

It is relevant to remark that the uncertainties of model parameters due to manufacturing process suggest to use the simplified model of Fig. 3 as an initial deterministic guess for the development of a stochastic description of a nanointerconnect.

4 Stochastic simulation of nanointerconnects

This Section summarizes the proposed procedure for the stochastic simulation of a nano interconnect described by the simplified equivalent of Fig. 3. For conciseness, the discussion is based on a single random parameter. The extension to the case or multiple random variables can be readily derived. The parameter selected to illustrate the method is the number n of metallic conductors in the bundle, that is one of the major sources of uncertainty. It is assumed to be uniformly distributed and defined by

$$n = (\frac{n_2 + n_1}{2}) + (\frac{n_2 - n_1}{2})\xi \tag{3}$$

where ξ is the normalized uniform random variable with support [-1,1] and n_1 and n_2 are the minimum and the maximum number of metallic conductors, respectively.

The proposed strategy is the following: (i) generate extended stochastic models of the different parts composing the cascaded structure that will be able to include the effects of the statistical variation of model parameters, i.e., of the stochastic parameter defined by (3), and (ii) simulate the entire structure in the frequency-domain by suitably concatenating these models.

In this study, the constitutive relations of the different cascaded blocks are represented in terms of their transmission matrix representations in the Laplace domain. The time-domain voltage and current variables $\{v_k, i_k\}$, $k = 1, \ldots, 4$ are replaced by $\{V_k, I_k\}$ and the source and load elements of Fig. 3 are assumed to be described by linear Thevenin equivalents.

4.1 Model of lumped blocks. Without parameter uncertainty, the constitutive relation of the two-port identical lumped elements defined by the series resistors of Fig. 3 is given by the transmission matrix representation $\mathbf{T}_1$. As an example, the electrical law governing the block on the left writes

$$\mathbf{X}_2 = \mathbf{T}_1\mathbf{X}_1 = \begin{bmatrix} 1 & -R_p/2n \\ 0 & 1 \end{bmatrix} \mathbf{X}_1 \tag{4}$$

where $\mathbf{X}_2 = [V_2, I_2]^T$ and $\mathbf{X}_1 = [V_1, I_1]^T$ are the vectors collecting the port variables. The same relation involving the port vectors $\mathbf{X}_4$ and $\mathbf{X}_3$ is used to represent the lumped block on the right.

When the problem becomes stochastic, i.e., with n defined by (3), we must consider the entries of (4) as random quantities. In turn, (4) becomes a stochastic equation leading to randomly-varying voltages and currents.

PC is a powerful tool allowing to solve in a clever way stochastic equations [8]. The idea behind this technique is the approximation of a random variable in terms of a truncated series of orthogonal polynomials that are functions of a predefined standard distribution. These polynomials play the same role as sinusoidal functions in the Fourier series expansion.

For the current application, both the voltage and current variables of (4) as well as the matrix $\mathbf{T}_1$ can be represented in terms of a truncated series. For instance,

$$\mathbf{T}_1 = \sum_{k=0}^{P} = \mathbf{T}_{1k}\phi_k(\xi) \tag{5}$$

where P is the order of the expansion that generally lies within the range $2 \div 10$ for practical applications and the $\mathbf{T}_{1k}$ matrices are the expansion coefficients with respect to the orthogonal components ϕ_k computed according to [8]. Briefly speaking, the above expansion terms can be computed via the projection of (4) onto the orthogonal polynomials ϕ_k by means of a properly defined inner product. As an example, for the case of uniform random variables, the orthogonal basis functions are the Legendre polynomials ϕ_0=1, ϕ_1=ξ, ϕ_2=$(\frac{3}{2}\xi^2 - \frac{1}{2})$,.... Readers are referred to [8, 10] and references therein for a comprehensive and formal discussion of polynomial chaos.

For a predefined order (e.g., P = 1), the use of equation (5), along with a similar expansion of the unknown voltage and current variables, yields a modified version of (4)

$$\begin{aligned}\mathbf{X}_{20}\phi_0(\xi) + \mathbf{X}_{21}\phi_1(\xi) = (\mathbf{T}_{10}\phi_0(\xi) + \mathbf{T}_{11}\phi_1(\xi)) \cdot \\ \cdot (\mathbf{X}_{10}\phi_0(\xi) + \mathbf{X}_{11}\phi_1(\xi))\end{aligned} \tag{6}$$

Projection of (6) on the first two Legendre polynomials leads to the following augmented system, where the random variable ξ does not appear, due to projection integral.

$$\begin{bmatrix} \mathbf{X}_{20} \\ \mathbf{X}_{21} \end{bmatrix} = \tilde{\mathbf{T}}_1 \begin{bmatrix} \mathbf{X}_{10} \\ \mathbf{X}_{11} \end{bmatrix} = \begin{bmatrix} \mathbf{T}_{10} & \frac{1}{3}\mathbf{T}_{11} \\ \mathbf{T}_{11} & \mathbf{T}_{10} \end{bmatrix} \begin{bmatrix} \mathbf{X}_{10} \\ \mathbf{X}_{11} \end{bmatrix} \tag{7}$$

According to the above equation, two new vectors $\tilde{\mathbf{X}}_1 = [\mathbf{X}_{10}, \mathbf{X}_{11}]^T$ and $\tilde{\mathbf{X}}_2 = [\mathbf{X}_{20}, \mathbf{X}_{21}]^T$ are defined to collect the different coefficients of the polynomial chaos expansion of the unknown variables.

It is worth noticing that equation (7) belongs to the same class of (4) and plays the role of the set of equations of a multiterminal circuit element, whose number of terminal is $(P+1)$ times larger than in the original circuit. However, for small values of P (as typically occurs in practice) the additional overhead in handling the augmented equations is much less than the time required to run a large number of MC simulations. The extension of equation (7) to the case of multiple random variables can be done by replacing the univariate polynomials in (5) with the corresponding multivariate polynomials, built as the product combinations of the univariate ones

4.2 Model of distributed lines. Similarly, the extended two-port description of the transmission line can be obtained via the projection of the telegraph equations governing the signal propagation along the single equivalent line of Fig. 3. The above projection leads to an extended set of multiconductor transmission-line equations, with augmented matrices $\mathbf{R}$, $\mathbf{L}$ and $\mathbf{C}$. Readers are referred to [11] for additional details on the extended model derivation. The augmented multiconductor equation is then used to generate the transmission matrix defining the extended characteristics $\tilde{\mathbf{T}}_2$ of block $\mathbf{T}_2$,

$$\tilde{\mathbf{X}}_3 = \tilde{\mathbf{T}}_2\tilde{\mathbf{X}}_2 = \mathrm{expm}\left(-\begin{bmatrix} 0 & \mathbf{R}+s\mathbf{L} \\ s\mathbf{C} & 0 \end{bmatrix}\mathcal{L}\right)\tilde{\mathbf{X}}_2 \tag{8}$$

where $\mathcal{L}$ is the line length and the interpretation of the new variables is straightforward.

4.3 Boundary conditions and simulation. Building on known facts, let us summarize that the simulation of an interconnect like the one of Fig. 3 amounts to combining the characteristics of the different circuit elements, including the driver and the receiver, and solving the system. When the two-port elements of Fig. 3 are defined by means of their transmission characteristics, the equivalent characteristics of the cascade connection of the three blocks is $\mathbf{T}_1\mathbf{T}_2\mathbf{T}_1$. Similarly, when the problem becomes stochastic, the augmented equations (7) and (8) are used in place of the deterministic ones together with the projection of the characteristics of the source and the load elements on the first P polynomials.

Once the unknown voltages and currents are computed, the quantitative information on the spreading of circuit responses can be readily obtained from the analytical expression of the unknowns. As an example, the frequency-domain solution of the magnitude of voltage V_4 with $P = 2$, leads to $|V_4(j\omega)| = |V_{40}(j\omega)\phi_0(\xi)+V_{41}(j\omega)\phi_1(\xi)+V_{42}(j\omega)\phi_2(\xi)|$. The above relation turns out to be a known nonlinear function of the random variable ξ that can be used to compute the PDF of $|V_4(j\omega)|$ via standard techniques as numerical simulation or analytical formulas.

5 Numerical results

In this Section, the proposed technique is applied to the analysis of the test structure of Fig. 3, that describes a $\mathcal{L} = 20\,\mu$m long SWCNT bundle placed over a ground plane at a distance $d = 100\,\mu$m. The driver of Fig. 3 is replaced by a Thevenin equivalent with a $25\,\Omega$ series impedance and a voltage source $E(s)$ (in the Laplace domain). Similarly, the receiver is replaced by a 10^{-2} pF capacitor that accounts for the dominant capacitive behavior of its input port.

The variability is provided by the number n of conducting tubes, that is assumed to behave as described by (3) with $n_1 = 20$ and $n_2 = 100$. The approximate relations of Sec. 4, are used to compute the fourth-order PC expansion of the unknowns and

of the parameters of the structure leading to (7) and (8). The equivalent electrostatic capacitance is $C_e = 18.51$ pF/m.

Figure 4 shows a comparison of the Bode plot (magnitude) of the transfer function $H(j\omega) = V_4(j\omega)/E(j\omega)$ computed via the advocated PC method and determined via the deterministic equations for a predefined value of n. Clearly, the accuracy of the proposed method in reproducing the large spreading of the reference responses of the interconnect for the possible different values of n can be appreciated form the curves of Fig. 4.

In order to provide a quantitative statistical information on the variability effects of system responses, Fig. 5 compares the PDF of $|H(j\omega)|$ computed for different frequencies over 40,000 MC simulations, and the distribution obtained form the analytical PC expansion of $H(j\omega)$. The frequencies selected for this comparison correspond to the vertical dashed lines shown in Fig. 4. The good agreement between the actual and the predicted PDFs and, in particular, the accuracy in reproducing the tails and the large variability of non-uniform shapes of the reference distributions, confirm the potential of the proposed method. In addition, for this example, it is also clear that a PC expansion with five terms is accurate enough to capture the dominant statistical information of the system response.

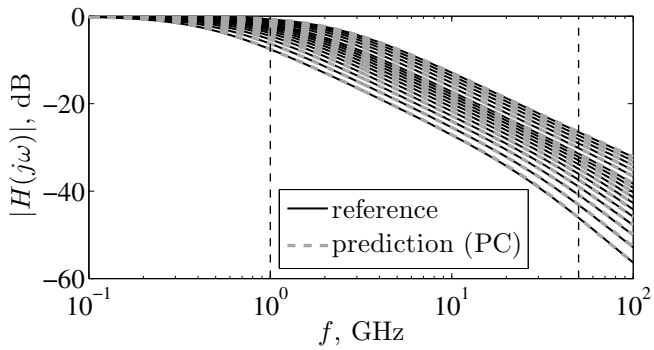

Figure 4: Bode plots (magnitude) of the transfer function $H(j\omega)$=$V_4(j\omega)/E(j\omega)$ of the example test case of this study (see text for details). Solid black thin lines: selection of the deterministic responses obtained by stepping n within the range $20 \div 100$; gray dashed lines: responses obtained via the proposed PC method.

The proposed method is faster by two orders of magnitude with respect to MC approach in computing the probability functions of Fig. 5. This holds even if for fairness we consider the computational overhead required by the solution of the augmented set of Equations (7) and (8). The above comparison confirms the strength of the proposed method, that allows to generate accurate predictions of the statistical behavior of a realistic interconnect with a great efficiency improvement.

It is important to remark that the PC technique can be effectively used without any modification of the method for a number of random variables on the order of ten. With a larger number of variables, the computation of the expansion coefficients requires the solution of multiple integrals, thus leading to an unavoidable initial overhead that is not negligible. In this case, a clever integration strategy needs to be used. Also, the size of

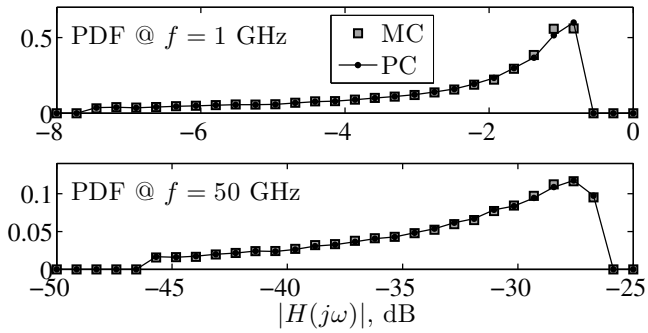

Figure 5: Probability density function of $|H(j\omega)|$ computed for two different frequencies. The distributions marked MC refers to 40000 MC simulations, and these marked PC refers to the response obtained via fourth-order polynomial chaos expansion.

the augmented set of equations defined by (7) and (8) increases with the number of variables. As an example, a third order expansion for the case of ten random variables leads to a system that is 286 times larger. Owing to this, if needed, possible model order reduction techniques can be combined with PC to improve the efficiency of the method

References

[1] V. N. Popov, "Carbon Nanotubes: Properties and Application", Materials Science and Engineering, Vol. 43, No. 3, pp. 61–102, Jan. 2004.

[2] S. Salahuddin, M. Lundstrom, S. Datta, "Transport Effects on Signal Propagation in Quantum Wires," IEEE Trans. on Electron Devices, Vol. 52, No. 8,pp. 1734–1742, Aug. 2005.

[3] A. Maffucci, "Carbon nanotubes in nanopackaging applications," IEEE Nanotechnology Magazine, Vol. 3 , No. 3, pp. 22–25, 2009.

[4] P. J. Burke, "An RF Circuit Model for Carbon Nanotubes," IEEE Trans. on Nanotechnology, Vol. 2, No. 1, pp. 55–58, Mar. 2003.

[5] A. Maffucci, G. Miano, F. Villone, "A Transmission Line Model for Metallic Carbon Nanotube Interconnect," Int. J. of Circ. Theory and Applications, Vol. 36, No. 1, pp. 31–51, Jan. 2008.

[6] M. D'Amore, M. S. Sarto, A. Tamburrano, "Fast Transient Analysis of Next-Generation Interconnects Based on Carbon Nanotubes," IEEE Trans. on EMC, Vol. 52, No. 2, May. 2010.

[7] C. R. Paul, "Analysis of Multiconductor Transmission Lines," Wiley, 1994.

[8] D. Xiu, G. E. Karniadakis, "The Wiener-Askey polynomial chaos for stochastic differential equations," SIAM, Journal of Sci. Computation, Vol. 24, No. 2, pp. 619–622, 2002.

[9] N. Wiener, "The homogeneous chaos", Amer. J. Math., Vol. 60, pp. 897–936, 1938.

[10] K. Strunz, Q. Su, "Stochastic formulation of SPICE-type electronic circuit simulation using polynomial chaos," ACM Transactions on Modeling and Computer Simulation, Vol. 18, No. 4, Sep. 2008.

[11] P. Manfredi, I. S. Stievano, F. G. Canavero, "Parameters Variability Effects on Microstrip Interconnects via Hermite Polynomial Chaos," Proc. of the *19th IEEE Conference on EPEPS*, Austin, TX, pp. 149–152, Oct. 25–27, 2010.